DALTON
FULL PAPER

Copper complexes with ferrocenyl pendants: Evidence for an $Fe^{II} \sim Cu^{II} \rightleftharpoons Fe^{III} \sim Cu^{I}$ electron transfer equilibrium leading to a reaction with dioxygen

Andrew J. Evans, Scott E. Watkins, Donald C. Craig and Stephen B. Colbran *

School of Chemistry, The University of New South Wales, Sydney, NSW 2052, Australia. E-mail: S.Colbran@unsw.edu.au

Received 12th June 2001, Accepted 21st December 2001
First published as an Advance Article on the web 15th February 2002

Three new nitrogen-donor ligands with ferrocenyl pendants, namely ferrocenylmethylbis(2-pyridylethyl)amine (L^1), ferrocenylmethylbis(2-pyridylmethyl)amine (L^2), and 1-ferrocenylmethyl-4,7-diisopropyl-1,4,7-triazacyclononane (L^3), have been synthesised. Copper(II) complexes of these ligands have been made and their physicochemical and redox properties characterised. Crystal structures of $[Cu(L^2)X_2 \cdot 0.5Et_2O$ (X = Cl, Br), $[Cu(L^2)(OTf)_2(CH_3OH)]$, $[Cu(L^3)Cl_2]$, and $[\{(L^3)Cu\}_2(\mu\text{-}OH)_2](OTf)_2 \cdot 0.5Et_2O$ are reported. Oxidation of each complex with ceric ion affords the corresponding $Fe^{III} \sim Cu^{II}$ species. Variations in ligand design, the choice of co-ligand (chloride, bromide, trifluoromethanesulfonate (OTf) or solvent) and the choice of solvent allowed, in the case of acetonitrile solutions of $[Cu(L^1)(H_2O)_2](OTf)_2$, the close matching of the Fe^{III}–Fe^{II} and Cu^{II}–Cu^{I} electrochemical couples. $[Cu(L^1)(H_2O)_2](OTf)_2$ reacts with dioxygen in acetonitrile, but is stable in other solvents such as tetrahydrofuran. Electronic spectra of the complex in acetonitrile exhibit a prominent ferrocenium ion band. These results are interpreted in terms of an intramolecular electron transfer equilibrium between $Fe^{II} \sim Cu^{II}$ and $Fe^{III} \sim Cu^{I}$ tautomers for the complex that leads to it reacting with dioxygen; their possible biological relevance is discussed.

Introduction

Copper amine oxidases (CAOs) are ubiquitous enzymes that occur in bacteria, yeasts, plants and animals where they regulate biogenic primary amine levels by catalysing their oxidation to the corresponding aldehydes.[1–10] Within the active sites of CAOs are a copper centre and an unusual quinone cofactor, TOPA-quinone (the quinone form of 2,4,5-trihydroxyphenylalanine),[2] derived by post-translational modification of a specific tyrosine residue.[3] In active CAOs the copper ion is bound by three histidine ligands and two water coligands and not by the TOPA-quinone cofactor;[4,5] a structurally characterised form with the cofactor coordinated to the copper ion is inactive.[4a] Oxidation of the primary amine substrates of these enzymes to the corresponding aldehyde takes place by Schiff base chemistry centred at the quinone cofactor and produces a reduced state with a copper(II) centre and the two-electron reduced, aminohydroquinone form of the cofactor.[6]

The mechanism of the re-oxidation of the reduced state of CAOs by dioxygen is more controversial. Temperature and cyanide dependent electron transfer equilibria within the active site between copper(II) ~ aminohydroquinone and copper(I) ~ aminosemiquinone centres have been observed for CAOs from several sources.[7] The electron transfer equilibria have catalytically competent rates,[7] leading to the proposal that the enzyme cycles are completed by dioxygen binding at the copper(I) centre, with concomitant oxidation of the copper and adjacent aminosemiquinone centres to regenerate copper(II) and the quinone cofactor.[1–8] The dioxygen would be reduced to and released as peroxide.[1–8] An EXAFS study of CAOs from several sources reveals the dithionite fully reduced state to exhibit three-coordinate copper centres, consistent with a role for copper(I) in the binding and reduction of dioxygen.[8] More recently, a dioxygen adduct of the CAO from *Escherichia coli* has been trapped at low temperature and its crystal structure determined—dioxygen appears bound as peroxide to copper, albeit at a long 2.8 Å.[5] However, a recent detailed kinetic study of bovine serum CAO (BSAO) provides evidence for a rate-limiting one-electron transfer from the reduced cofactor to dioxygen bound at a site separate from the copper site.[9] Moreover, metal replacement studies of *Hansenula polymorpha* CAO suggest that copper may not be essential; activity is maintained when cobalt replaces copper.[10] These results throw doubt on the role of the copper ion (in these CAOs at least), suggesting that it is not the (initial) binding site for dioxygen and that it does not have a redox role as previously presumed. Thus, there remains some mechanistic ambiguity for the reaction of the reduced enzyme with dioxygen, and it may be that CAOs from different sources differ in the mechanism of re-oxidation of the reduced, aminohydroquinone form of the cofactor.[3]

The feasibility of a proposed step in a suggested enzyme mechanism can be tested by model studies. For example, Kaim and colleagues recently demonstrated a temperature-dependent equilibrium between the valence tautomers of some copper complexes with redox active *o*-semiquinone/*o*-hydroquinone (catecholate) chelate ligands, eqn. 1.[11] The report is the first to

$$LCu^{II}(O,O'\text{-}o\text{-hydroquinone}) \rightleftharpoons LCu^{I}(O,O'\text{-}o\text{-semiquinone}) \quad (1)$$

describe an intramolecular electron transfer equilibrium in simple copper model complexes akin to that in CAOs. The model complexes have the redox active *o*-(hydro/semi)quinone ligands directly bound to copper, unlike in the proteins where the quinone cofactor is not bound to copper, and whether they react with dioxygen was not described. Also recently, Halcrow and co-workers have shown that formation of Schiff bases provides a facile route to copper(II) complexes substituted by hydroquinones; unfortunately the complexes do not survive oxidation.[12] Likewise, a copper(II) complex of the monoanion from 2-hydroxy-5-methyl-1,4-benzoquinone, prepared as a

DOI: 10.1039/b105150b

model for the TOPA-quinone on copper form of CAOs, decomposes upon reduction.[13] There is little other model chemistry for the copper–*p*-quinone centres in CAOs.[14]

Inspired by the above biological copper chemistry, we describe herein the synthesis and (spectro)electrochemical characterisation of a series of copper complexes of three new ferrocenyl-substituted ligands with bis(2-pyridylethyl)amine (bpea), bis(2-pyridylmethyl)amine (bpma) and tris(alkylated)-triazacyclononane (R_3tacn) copper-binding domains, Chart 1.

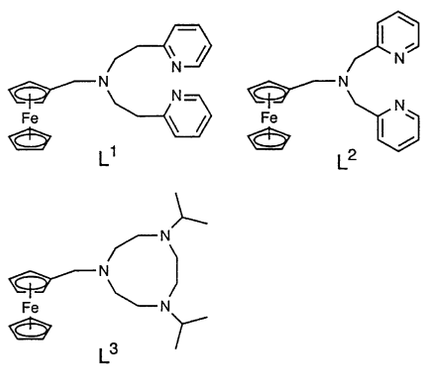

Chart 1

Copper(I) complexes of these nitrogen-donor ligand domains bind and activate dioxygen.[15–17] The ferrocenyl pendant is not intended to model the TOPA-quinone cofactor in CAOs, rather it should be considered a surrogate auxiliary electron donor. The study of these ferrocenyl–copper complexes provides evidence for an electron transfer equilibrium which mimics that in CAOs from the reduced cofactor to the copper, and reveals an interesting interplay between the redox potentials of the copper and the auxiliary electron donor centres, the thermodynamics of the electron transfer equilibrium and dioxygen binding by the copper centre.

Experimental

Physical measurements

Elemental analyses for C, H and N were determined by the Australian National University Microanalytical Unit. Elemental ratios for Cu, Fe and S are calculated from inductively-coupled plasma–atomic emission spectroanalysis (ICP–AES) data. Samples for ICP–AES were prepared by digestion of the complex with 10% nitric acid overnight; the individual concentrations of Cu, Fe and S in the samples were then simultaneously determined (reproducible to ±10%) using a GBC Integra ICP–AES instrument fitted with a 22-channel polychromator. Electrospray mass spectra (ES-MS) were acquired on a VG Quattro mass spectrometer with a capillary voltage of 4 kV and a cone voltage of 30 V. The solvent system was 50 : 50 acetonitrile–water with 1% acetic acid. ^{1}H NMR spectra were recorded on a Bruker AC 300F (300 MHz) spectrometer. Room temperature magnetic moments were determined on a magnetic susceptibility balance using the Gouy method. Diamagnetic corrections were calculated from tabulated values of Pascal's constants. Molar conductivity measurements were made on ~1 mM solutions of the complexes in acetonitrile at 25 °C. The molar conductivity of the 1 : 1 electrolyte tetra-*n*-butylammonium hexafluorophosphate was determined to be 157 S cm^2 mol^{-1} under these conditions. Electronic spectra of complexes were recorded between 300 and 2000 nm on a CARY 5 spectrometer in the dual beam mode; solution spectra were recorded in sealed 1 cm quartz cuvettes and solid state spectra were recorded as KBr disks. Solutions of $[Cu(L^1)(H_2O)_2](CF_3SO_3)_2$ under nitrogen were prepared in a M. Braun glovebox operating with dioxygen and water levels below 2 ppm. EPR spectra were recorded for both frozen solution (at 77 K; liquid nitrogen dewar) and solid (dispersed in a KBr matrix) samples using a Bruker EMX 10 EPR spectrometer. Mössbauer spectra were recorded in transmission mode with a constant acceleration spectrometer at room temperature equipped with a ^{57}Co/Pd source and a Wissel drive unit with associated Ortec electronics. The velocity scale was calibrated with metallic iron foil and sodium nitroferricyanide(III), and the isomer shift value quoted is relative to the mid-point of the iron spectrum at room temperature. The spectral parameters were extracted from a least squares fit of the data to Lorentzian line shapes. Electrochemical measurements were recorded using a Pine Instrument Co. AFCBP1 bipotentiostat interfaced to and controlled by a Pentium computer. For cyclic voltammetry measurements, a standard three electrode configuration was used with a quasi-reference electrode comprised of a commercial Ag–AgCl mini-reference electrode (Cyprus Systems, Inc. EE008) but filled with the same electrolyte solution as used in the experiment [rather than saturated AgCl in 3 M KCl(aq) solution], a freshly polished platinum disk (1 mm diameter) working electrode and a platinum wire as the auxiliary electrode.[18] Solutions of the compounds were 1.0 mM in anhydrous acetonitrile (Aldrich, used as received) with 0.1 M tetra-*n*-butylammonium hexafluorophosphate. Data are reported from cyclic voltammograms recorded at a scan rate of 100 mV s^{-1}. Except where stated otherwise, the electrochemical potentials quoted in this paper are relative to the ferrocene-ferrocenium (Fc^+–Fc) couple measured under the same experimental conditions (same concentrations, solvent, support electrolyte, electrodes, temperature and scan rate).[19]

Syntheses

Reactions carried out under an atmosphere of dry nitrogen were performed using standard Schlenk and cannula techniques. Dry solvents were obtained by routine distillation from the appropriate drying agent under nitrogen immediately prior to use: acetonitrile from P_2O_5, methanol from magnesium turnings activated with iodine, diethyl ether and tetrahydrofuran from sodium benzophenone. Flash chromatography was carried out using Merck silica gel 7730 60GF_{254} as the support. Columns were packed with dry gel; solvent was applied to the column before a concentrated solution of the sample in the appropriate solvent. A water aspirator was attached to the receiving flask during packing and elution. The ligand precursors, ferrocenylmethyltrimethylammonium iodide,[20] *N,N′*-bis(2-pyridylethyl)amine (bpea),[21] *N,N′*-bis(2-pyridylmethyl)-amine (bpma),[22] and 1,4-diisopropyl-1,4,7-triazacyclononane (Pr^i_2tacn)[23] were prepared according to methods outlined in the literature. Table 1 presents partial elemental analytical, ICP–AES, and ES-MS data for the complexes. Data from electronic and EPR spectra, and from conductivity measurements are given in Table 2.

Ferrocenylmethylbis(2-pyridylethyl)amine (L^1). Freshly prepared $[FcCH_2NMe_3]I$ (11.99 g, 0.031 mol) was added to a solution of bpea (7.05 g, 0.031 mol) in deoxygenated water (150 mL) and the solution refluxed under N_2 for 13 h. The red–brown oil which had separated was extracted with diethyl ether (4 × 100 mL) and the organic layer was dried over anhydrous sodium sulfate. The solution was filtered, evaporated and dried *in vacuo* (for 5 h @ 0.1 mm Hg), yielding L^1 as a thick red–brown oil, which was used without further purification (9.24 g, 70%). (Found: C, 70.31; H, 6.50; N, 10.02%. $C_{25}H_{27}FeN_3$ requires C, 70.59; H, 6.40; N, 9.88%.) ES-MS *m*/*z*: 426 (L^1H^+). ^{1}H NMR ($CDCl_3$): δ 8.49 (dd, J_{HH} = 5.13 and 2.04 Hz, pyH, 2H), 7.52 (td, J_{HH} = 7.20 and 2.04 Hz, pyH, 2H), 7.07 (m, pyH, 4H), 4.15 (m, C_5H_4, 2H), 4.08 (m, C_5H_4, 2H and C_5H_5, 5H), 3.60 (s, CH_2, 2H), 2.88 (m, CH_2CH_2, 8H). UV-Vis (MeCN) λ_{max}/nm (10^{-3} ε/M^{-1} cm^{-1}): 415 (0.22), 328 (0.64).

Table 1 Colours, yields, and analytical and mass spectral data for the complexes

Complex	Colour and form	Yield (%)	Found (%)	Calc. (%)	ICP–AES Cu : Fe (: S)	ES-MS m/z (% full scale)
$[Cu(L^1)Cl_2]$	Dark green crystals (platelets)	38	C, 51.99 H, 4.92 N, 7.17	$C_{25}H_{27}Cl_2CuFeN_3\cdot H_2O$ C, 51.96 H, 5.06 N, 7.27	1.00 : 0.95	426 (100) L^1H^+ 488 (1) L^1Cu^+ 523 (10) L^1CuCl^+ 547 (5) L^1CuOAc^+
$[Cu(L^1)Br_2]$	Green powder	73	C, 45.13 H, 4.19 N, 6.25	$C_{25}H_{27}Br_2CuFeN_3\cdot H_2O$ C, 45.03 H, 4.23 N, 6.30	1.00 : 0.96	426 (100) L^1H^+ 488 (5) L^1Cu^+ 547 (5) L^1CuOAc^+ 567 (10) L^1CuBr^+
$[Cu(L^1)(H_2O)_2](OTf)_2$	Black crystals (needles)	66	C, 38.72 H, 3.71 N, 5.08	$C_{27}H_{27}CuF_6FeN_3O_6S_2\cdot 2H_2O$ C, 39.40 H, 3.80 N, 5.11	1.00 : 0.96 : 1.64	426 (100) L^1H^+ 488 (40) L^1Cu^+ 547 (20) L^1CuOAc^+ 637 (30) $L^1CuOSO_2CF_3^+$
$[Cu(L^2)Cl_2]$	Green crystals (platelets)	70	C, 51.61 H, 4.91 N, 7.36	$C_{23}H_{23}Cl_2CuFeN_3$ C, 51.95 H, 4.36 N, 7.90	1.00 : 0.88	230 (10) L^2Cu^{2+} 398 (1) L^2H^+ 495 (100) L^2CuCl^+ 519 (5) L^2CuOAc^+ 1025 (10) $L^2{}_2Cu_2Cl_3^+$
$[Cu(L^2)Br_2]$	Green powder Green crystals (platelets)	41 32	C, 44.82 H, 3.64 N, 6.81	$C_{23}H_{23}Br_2CuFeN_3$ C, 44.51 H, 3.74 N, 6.77	1.00 : 0.96	230 (20) L^2Cu^{2+} 460 (5) L^2Cu^+ 519 (5) L^2CuOAc^+ 539 (100) L^2CuBr^+ 1157 (20) $L^2{}_2Cu_2Br_3^+$
$[Cu(L^2)(H_2O)_2](OTf)_2$	Dark blue/green crystal	74	C, 37.93 H, 3.07 N, 5.46	$C_{25}H_{23}CuF_6FeN_3O_6S_2\cdot 2H_2O$ C, 37.77 H, 3.42 N, 5.29	1.00 : 0.94 : 1.60	230 (100) L^2Cu^{2+} 460 (20) L^2Cu^+ 519 (30) L^2CuOAc^+ 609 (80) $L^2CuOSO_2CF_3^+$ 1369 (5) $L^2{}_2Cu_2(OSO_2CF_3)_3^+$
$[Cu(L^3)Cl_2]$	Light green crystals (prisms)	23	C, 50.57 H, 6.97 N, 7.36	$C_{23}H_{37}Cl_2CuFeN_3$ C, 50.60 H, 6.83 N, 7.70	1.00 : 0.98	412 (20) L^3H^+ 474 (30) L^3Cu^+ 509 (70) L^3CuCl^+ 533 (100) L^3CuOAc^+ 1053 (5) $L^3{}_2Cu_2Cl_3^+$
$[\{(L^3)Cu\}_2(\mu\text{-}OH)_2](OTf)_2$	Bright green crystals (platelets)	22	C, 43.40 H, 6.11 N, 6.49	$C_{48}H_{76}Cu_2F_6Fe_2N_6O_8S_2$ C, 44.96 H, 5.98 N, 6.56	1.00 : 0.88 : 0.82	533 (100) L^3CuOAc^+

Table 2 Vis-NIR, X-band EPR (77 K) spectroscopic and molar conductivity (for 1.0 mM solutions) data for the complexes; all data are for acetonitrile solutions except where indicated otherwise

Complex	Vis-NIR λ_{max}/nm ($10^{-3}\varepsilon$/L mol^{-1} cm^{-1})	EPR	Molar conductivity Λ_M/S cm^2 mol^{-1}
$[Cu(L^1)Cl_2]$	454 (0.20), 798 (0.38), 1002 (sh, 0.25)	$g_\parallel$ 2.23 ($A_\parallel$ 147 G), $g_\perp$ 2.12	18
$[Cu(L^1)Br_2]$	772 (0.60), 1010 (sh, 0.30)	g_{iso} 2.19 (br)	50
$[Cu(L^1)(H_2O)_2](OTf)_2$	628 (0.83) 491 (0.41),[a] 671 (0.66)[a]	$g_\parallel$ 2.25 ($A_\parallel$ 152 G), $g_\perp$ 2.07	275
$[Cu(L^2)Cl_2]$	455 (0.20), 742 (0.20), 1020 (sh, 0.10)	$g_\parallel$ 2.22 ($A_\parallel$ 175 G), $g_\perp$ 2.09	42
$[Cu(L^2)Br_2]$	454 (0.19), 751 (0.29), 980 (sh, 0.19)	g_{iso} 2.11(br)	62
$[Cu(L^2)(H_2O)_2](OTf)_2$	462 (0.16), 595 (0.23)	$g_\parallel$ 2.25 ($A_\parallel$ 180 G), $g_\perp$ 2.06	[b]
$[Cu(L^3)Cl_2]$	727 (0.11), 1183 (0.04)	$g_\parallel$ 2.27 ($A_\parallel$ 151 G), $g_\perp$ 2.05	47
$[\{(L^3)Cu\}_2(\mu\text{-}OH)_2](OTf)_2$	638 (0.13), 977 (0.06)	Silent	[b]

[a] In tetrahydrofuran solution. [b] Not measured.

Ferrocenylmethylbis(2-pyridylmethyl)amine (L^2). Freshly prepared $[FcCH_2NMe_3]I$ (6.05 g, 0.016 mol) was added to a solution of bpma (3.12 g, 0.016 mol) in deoxygenated water (100 mL) and the solution refluxed under N_2 for 14 h. The red oil which formed was extracted with diethyl ether (4 × 100 mL) and the organic layer was dried over anhydrous sodium sulfate. The solution was filtered, evaporated and dried *in vacuo* (for 6 h @ 0.1 mm Hg) to afford orange–brown crystals of L^2 (4.59 g, 72%). (Found: C, 69.57; H, 5.75; N, 10.69%. $C_{23}H_{23}FeN_3$ requires C, 69.53; H, 5.84; N, 10.58%.) ES-MS *m/z*: 398 (L^2H^+). ^{1}H NMR ($CDCl_3$): δ 8.52 (d, J_{HH} = 4.62 Hz, pyH, 2H), 7.64 (td, J_{HH} = 7.70 and 2.04 Hz, pyH, 2H), 7.53 (d, J_{HH} = 7.70 Hz, pyH, 2H), 7.13 (dd, J_{HH} = 7.70 and 4.62 Hz, pyH, 2H), 4.20 (t, C_5H_4, 2H), 4.10 (d, C_5H_4, 2H), 4.02 (s, C_5H_5, 5H), 3.78 (s, CH_2, 4H), 3.58 (s, CH_2, 2H). UV-Vis (MeCN) λ_{max}/nm (10^{-3} ε/M^{-1} cm^{-1}): 433 (0.12), 329 (0.23).

1-Ferrocenylmethyl-4,7-diisopropyl-1,4,7-triazacyclononane (L^3). Freshly prepared $[FcCH_2NMe_3]I$ (3.16 g, 0.0082 mol) was added to a solution of $Pr^i{}_2$tacn (1.75 g, 0.0082 mol) in deoxygenated water (100 mL) and the solution refluxed under N_2 for 6 h. After extraction of the reaction mixture with diethyl ether (3 × 100 mL), the dark brown solid which separated from the aqueous layer was collected and dried *in vacuo* (for 3 h @ 0.1 mm Hg), yielding $[HL^3]I$, the iodide salt of the protonated ligand (0.88 g, 20%). (Found: C, 50.08; H, 7.08; N, 7.29%. $C_{23}H_{38}FeIN_3\cdot H_2O$ requires C, 49.56; H, 7.23; N, 7.54%.) ES-MS *m/z*: 412 (L^3H^+). ^{1}H NMR ($CDCl_3$): δ 4.17 (d, FcH, 9H), 3.71

(s, CH_2, 2H), 2.95 (br m, tacn, 12H and CH, 2H), 1.12 (m, CH_3, 12H). CV: $E_{1/2}$ (Fe^{III}–Fe^{II}) = 34 mV. The organic layer was dried over anhydrous sodium sulfate, filtered, and the solvent removed by rotary evaporation. The resulting oil was purified by flash chromatography (silica column; CH_2Cl_2–MeOH gradient) to give L^3 as a brown oil (1.27 g, 38%). ^{1}H NMR ($CDCl_3$): δ 4.15 (m, FcH, 9H), 3.70 (s, CH_2, 2H), 2.95 (br m, tacn, 12H and CH, 2H), 1.09 (d, CH_3, 12H). UV-Vis (MeCN) λ_{max}/nm (10^{-3} ε/M^{-1} cm^{-1}): 417 (0.24), 319 (0.97).

[Cu(L^1)Cl_2]. A green solution of $CuCl_2 \cdot 2H_2O$ (106 mg, 0.62 mmol) in methanol (5 mL) was added to a stirred brown solution of L^1 (264 mg, 0.62 mmol) in methanol (5 mL). The solution of L^1 immediately turned dark blue/green and was stirred for 1 h. The solution was then placed in a diethyl ether atmosphere for 3 d, yielding green platelets of [Cu(L^1)Cl_2] (133 mg, 38%).

[Cu(L^1)Br_2]. A dark brown–yellow solution of anhydrous $CuBr_2$ (153 mg, 0.69 mmol) in methanol (5 mL) was added to a stirred brown solution of L^1 (293 mg, 0.69 mmol) in methanol (5 mL). The solution turned green and a dark green solid precipitated immediately. The solution was stirred for 1 h then filtered to yield [Cu(L^1)Br_2] as a green powder (326 mg, 73%).

[Cu(L^1)(H_2O)$_2$](OTf)$_2$. A pale blue solution of anhydrous $Cu(OSO_2CF_3)_2$ (Cu(OTf)$_2$, 260 mg, 0.72 mmol) in methanol (5 mL) was added to a stirred brown solution of L^1 (306 mg, 0.72 mmol) in methanol (5 mL) under N_2. The solution immediately turned dark blue and was stirred for 1 h. The solution was then placed in a diethyl ether atmosphere for 3 d, yielding black crystals (needles) of [Cu(L^1)(H_2O)$_2$](OTf)$_2$ (375 mg, 66%).

[Cu(L^2)Cl_2]. A lime green solution of anhydrous $CuCl_2$ (92 mg, 0.68 mmol) in dry methanol (5 mL) was added to a stirred dark brown solution of L^2 (272 mg, 0.68 mmol) in dry methanol (5 mL) under N_2. The solution of L^2 immediately turned dark green and was stirred for 1 h. The solution was then placed in a diethyl ether atmosphere for 3 d, yielding X-ray quality green crystals (platelets) of [Cu(L^2)Cl_2] (290 mg, 70 %).

[Cu(L^2)Br_2]. A dark brown–yellow solution of anhydrous $CuBr_2$ (156 mg, 0.70 mmol) in dry methanol (5 mL) was added to a stirred dark brown solution of L^2 (279 mg, 0.70 mmol) in dry methanol (5 mL) under N_2. The solution turned dark green/blue and a green solid precipitated from solution immediately. The solution was stirred for 1 h then filtered to yield [Cu(L_2)Br_2] as a green powder (180 mg, 41 %). The filtrate was placed in a diethyl ether atmosphere for 3 d, yielding X-ray quality green crystals of [Cu(L^2)Br_2] (137 mg, 32 %).

[Cu(L^2)(H_2O)$_2$](OTf)$_2$. A pale blue solution of anhydrous Cu(OTf)$_2$ (76 mg, 0.21 mmol) in methanol (5 mL) was added to a stirred dark brown solution of L^2 (84 mg, 0.21 mmol) in methanol (5 mL) under N_2. The solution immediately turned dark green and was stirred for 1 h. The solution was then placed in a diethyl ether atmosphere for 3 d, yielding dark blue/green crystals of [Cu(L^2)(H_2O)$_2$](OTf)$_2$ (123 mg, 74 %). Recrystallisation of this product from anhydrous methanol–diethylether solution afforded X-ray quality crystals of [Cu(L^2)(CH_3OH)-(OTf)$_2$].

[Cu(L^3)Cl_2]. A green solution of $CuCl_2 \cdot 2H_2O$ (59 mg, 0.35 mmol) in methanol (5 mL) was added to a stirred brown solution of L^3 (144 mg, 0.35 mmol) in methanol (5 mL). The solution immediately turned dark green and was stirred for 1 h. The solution was then placed in a diethyl ether atmosphere for 3 d, yielding light green prisms of [Cu(L^3)Cl_2] (44 mg, 23 %).

[{(L^3)Cu}$_2$(μ-OH)$_2$](OTf)$_2$. A pale blue solution of anhydrous Cu(OTf)$_2$ (202 mg, 0.56 mmol) in methanol (5 mL) was added to a stirred brown solution of L^3 (230 mg, 0.56 mmol) in methanol (5 mL). The solution immediately turned dark green and was stirred for 1 h. The solution was then placed in a diethyl ether atmosphere for 3 d, yielding bright green X-ray quality crystals of [{(L^3)Cu}$_2$(μ-OH)$_2$](OTf)$_2$ (78 mg, 22 %).

Oxidation of the copper complexes with ceric ion

General method: A yellow/orange solution of $(NH_4)_2Ce(NO_3)_6$ in acetonitrile (0.01 mmol) was added to a pale green solution of the complex (0.01 mmol) in acetonitrile (5 mL). The solution immediately turned an intense dark blue/green colour, and the Vis-NIR and EPR spectra were recorded immediately. The EPR spectra show only weak residual signals (10^2–10^3-fold less intense) for the starting complex. Vis-NIR spectra after addition of ceric ion; quoted are the initial complex and λ_{max} (MeCN)/nm (10^{-3} ε/M^{-1} cm^{-1}): **[Cu(L^1)Cl_2]** 465 (0.33), 634 (0.61), 759 (0.36), 960 (sh, 0.29); **[Cu(L^1)Br_2]** 639 (0.58), 756 (0.54), 960 (sh, 0.27); **[Cu(L^1)(H_2O)$_2$](OTf)$_2$** 450 (sh, 0.30), 630 (0.48); **[Cu(L^2)Cl_2]** 461 (0.21), 635 (0.41), 730 (sh, 0.12); **[Cu(L^2)Br_2]** 462 (0.56), 637 (0.49), 738 (0.28), 970 (sh, 0.15); **[Cu(L^2)(H_2O)$_2$](OTf)$_2$** 463 (0.25), 631 (0.51); **[Cu(L^3)Cl_2]** 634 (0.41), 730 (sh, 0.14), 1147 (0.08); **[{(L^3)Cu}$_2$(μ-OH)$_2$](OTf)$_2$** 631 (0.48).

X-Ray crystallography

Relevant crystal and refinement data are collected in Table 3. Although the geometry of each complex is well defined, the data collected for the structures described in this paper are generally weak, with the data range limited by unobservable reflections at higher angles caused by the crystal habit (and content).

CCDC reference numbers 166078–166082.

See http://www.rsc.org/suppdata/dt/b1/b105150b/ for crystallographic data in CIF or other electronic format.

Results and discussion

Ligand syntheses

The reactions of ferrocenylmethyltrimethylammonium iodide and *N*,*N*-bis(2-pyridylethyl)amine or *N*,*N*-bis(2-pyridylmethyl)-amine, in deoxygenated water under dinitrogen, afforded the ligands L^1 (a thick red–brown oil) and L^2 (an orange–brown solid), respectively (Chart 1). The analogous reaction of ferrocenylmethyltrimethylammonium iodide and 1,4-diisopropyl-1,4,7-triazacyclononane (Pr^i_2tacn) gave [HL^3]I (a brown solid), the iodide salt of the protonated ligand, which precipitated from the aqueous reaction mixture and was collected by filtration. Extraction of the filtrate with diethyl ether, followed by flash chromatography yielded L^3 (a brown oil).[24]

Ligands L^1–L^3 exhibited consistent elemental analyses, electrospray mass spectra and ^{1}H NMR spectra. The electronic spectra (300–2000 nm) of the ligands in acetonitrile solution show two absorbance bands, one at 320–330 nm in the rising tail of a UV-band to higher energy and a broad band at 415–440 nm ($\varepsilon \approx$ 120–240 M^{-1} cm^{-1}). These are likely ferrocene-centred transitions [for comparison, the two lowest energy transitions for ferrocene are at 325 nm ($\varepsilon \approx 52$ M^{-1} cm^{-1}) and 440 nm ($\varepsilon \approx 92$ M^{-1} cm^{-1})[25]]. It is relevant that no peak was observed for the ferrocenium (Fe^{III}) ion (which typically gives a sharp, intense peak at about 630 nm[25]) and that the ^{1}H NMR spectra have sharp peaks, indicating that the ligands were obtained in their reduced (Fe^{II}) state. Cyclic voltammograms (CVs) of the ligands in acetonitrile–0.1 M tetrabutylammonium hexafluorophosphate show electrochemically reversible, ferrocenyl-centred Fe^{III}–Fe^{II} couples at −28 mV for L^1, −8 mV for L^2 and +8 mV for L^3.

Table 3 Numerical crystal and refinement data for the X-ray crystal structures

Complex	$[Cu(L^2)Cl_2]\cdot 0.5Et_2O$	$[Cu(L^2)Br_2]\cdot 0.5Et_2O$	$[Cu(L^3)Cl_2]$	$[Cu(L^2)(OTf)_2(CH_3OH)]$	$[\{(L^3)Cu\}_2(\mu\text{-}OH)_2](OTf)_2\cdot 0.5Et_2O$
Formula (sum)	$C_{25}H_{28}Cl_2CuFeN_3O_{0.5}$	$C_{25}H_{28}Br_2CuFeN_3O_{0.5}$	$C_{23}H_{37}Cl_2CuFeN_3$	$C_{26}H_{27}CuF_6FeN_3O_7S_2$	$C_{25}H_{40.5}CuF_3FeN_3O_{4.25}S$
M	568.8	657.7	545.9	791.0	659.6
Crystal system	Monoclinic	Monoclinic	Monoclinic	Monoclinic	Monoclinic
Space group	$P2_1/c$	$P2_1/c$	$P2_1/c$	$P2_1/c$	$C2/c$
a/Å	13.192(6)	13.336(11)	7.116(3)	17.599(14)	31.627(36)
b/Å	11.449(4)	11.555(3)	29.896(11)	10.318(3)	10.993(8)
c/Å	16.718(6)	16.990(14)	13.696(6)	16.979(12)	20.899(23)
β/°	95.90(2)	96.20(4)	120.87(2)	96.57(4)	123.94
V/Å^3	2512(2)	2603(3)	2501(2)	3063(4)	6028(9)
Z	4	4	4	4	8
μ/cm^{-1} (Mo-Kα)	16.61	44.37	16.63	13.83	13.06
Reflections collected	2822	4774	4581	2083	2875
R_{merge} (no. of equiv. reflections)	0.012 (58)	0.022 (210)	0.020 (190)	0.018 (120)	0.027 (68)
Observed reflections $[I/\sigma(I) > 3]$	1913	2333	2907	1389	1574
Final R, R_w $[I/\sigma(I) > 3]$	0.028, 0.036	0.043, 0.054	0.035, 0.046	0.067, 0.115	0.062, 0.080

Ferrocenyl–copper complexes

Syntheses. Copper complexes of L^1–L^3 were prepared by combining the appropriate ligand and copper(II) salt [chloride, bromide or trifluoromethanesulfonate (OTf)] in methanol, and placing the resulting dark green–blue solution under a diethyl ether atmosphere. The (micro)crystalline products which formed were characterised by elemental analysis, ICP–AES, ES-MS (Table 1), Vis-NIR and EPR spectroscopies, molar conductivity measurements (Table 2), and X-ray crystallography (Table 3). The low values for sulfur in the Cu : Fe : S ratios from the ICP–AES analyses of the trifluoromethanesulfonate complexes are consistent with loss of volatile sulfur species (SO_2 and SO_3) during the oxidative sample preparation procedure (see Experimental section). The ES mass spectra of the complexes reveal peaks due to the $LCuX^+$ (X = Cl, Br or OTf) molecular ions as well as LCu^{2+}, LCu^+ and LH^+ ions. In addition, weak peaks for $L_2Cu_2X_3^+$ clusters from gas phase aggregation reactions are also observed.

Crystal structures. The crystal structures of $[Cu(L^2)X_2]\cdot 0.5Et_2O$ (X = Cl, Br), $[Cu(L^2)(OTf)_2(CH_3OH)]$, $[Cu(L^3)Cl_2]$, and $[\{(L^3)Cu\}_2(\mu\text{-}OH)_2](OTf)_2\cdot 0.5Et_2O$ are reported here; that of $[Cu(L^1)Cl_2]$ will be reported elsewhere.[26] Crystal and refinement data are given in Table 3.

$[Cu(L^2)Cl_2]\cdot 0.5Et_2O$ and $[Cu(L^2)Br_2]\cdot 0.5Et_2O$. In $[Cu(L^2)Cl_2]$, the copper ion is bound by the three nitrogen atoms of the ligand and two chloride ions in an almost perfect square pyramidal arrangement; the trigonality index (τ value) is 0.03 [for five co-ordinate complexes, $\tau = \alpha - \beta/60$ where α and β are the largest and next largest bond angles about the copper ion;[27] τ is 0 for a perfect square pyramid and 1.0 for a perfect trigonal bipyramid and for this complex α is 162.4(1)° and β is 160.9(1)°], Fig. 1. The base of the square pyramid is formed by the three nitrogen atoms of the ligand [Cu–N_{py} = 1.997(3) and 1.993(3) Å, Cu–N_{amine} = 2.062(3) Å] and one of the chloride ions [Cu–Cl_2 = 2.255(1) Å]. The other chloride ion bonds copper at the apex of the square pyramid, along the weak field axis [Cu–Cl1 = 2.581(1) Å]. $[Cu(L^2)Br_2]$ is isostructural with $[Cu(L^2)Cl_2]$, the only differences of note being the Cu–Br bond lengths [Cu–Br2 2.398(1) Å, Cu–Br1 2.750(1) Å], which as expected are longer than the Cu–Cl bond lengths. For $[Cu(L^2)Br_2]$ τ is 0.02 [α 162.8(3)°, β 161.7(2)°]. The copper centres are similar to those previously reported for a copper(II) ion bound by a bis(pyridylmethyl)amine domain and two chloro[28] or bromo[29] co-ligands. Normal bond distances {Fe–$C_{average}$ is 2.032 Å for $[Cu(L^2)Cl_2]$ and 2.023 Å for $[Cu(L^2)Br_2]$} and angles are observed for the ferrocene moiety.[30] However, the ferrocenyl group eclipses a pyridyl ring, Fig. 1. For $[Cu(L^2)Cl_2]$ the closest (non-hydrogen) distances between the pyridyl ring and the ferrocene are C8 ··· C14 3.034 Å, N2 ··· C14 3.167 Å, and C8 ··· C15 3.196 Å; the corresponding distances in $[Cu(L^2)Br_2]$ are 3.069 Å, 3.186 Å and 3.186 Å. In contrast, the ferrocenyl group is orientated away from the copper centre in the other structures reported in this paper and in the structure of $[Cu(L^1)Cl_2]$.[26]

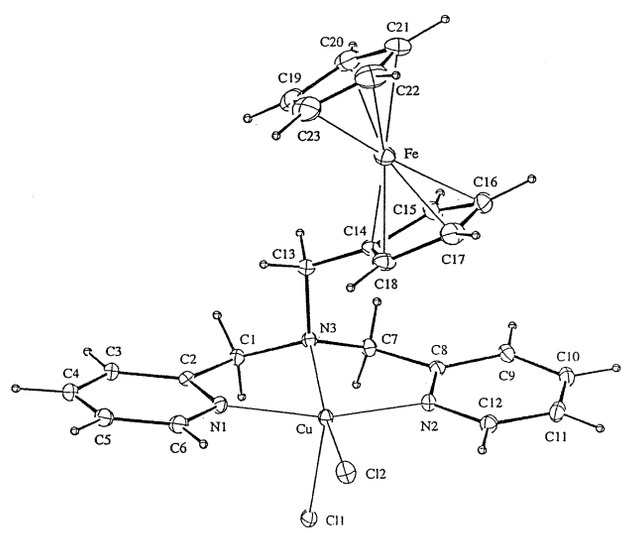

Fig. 1 View of $[Cu(L^2)Cl_2]$ (10% thermal ellipsoids at 294 K).

$[Cu(L^2)(OTf)_2(CH_3OH)]$. Recrystallisation of $[Cu(L^2)(H_2O)_2](OTf)_2$ from anhydrous methanol–diethylether solution afforded dark blue–green crystals of $[Cu(L^2)(OTf)_2(CH_3OH)]$, Fig. 2. The copper ion is bound at typical copper(II)–ligand bond distances[12–17,27–29] by the three nitrogen atoms of the ligand [Cu–N_{py} 1.971(11) and 1.969(12) Å, Cu–N_{amine} 2.032(11) Å] and by the oxygen atom of a methanol ligand [Cu–O_{MeOH} 2.037(11) Å]. Also two trifluoromethanesulfonate ions are weakly bound [Cu–O_{OTf} 2.327(8) and 2.615(8) Å] to give the complex a tetragonally-elongated octahedral geometry; one trifluoromethanesulfonate ion, that towards the ferrocene moiety, is two-fold disordered in the structure. Key bond angles about the copper ion are: N_{amine}–Cu–O_{MeOH} 163.5(6)°, N_{py}–Cu–$_{py'}$ 166.4(4)° and O_{OTf}–Cu–$O_{OTf'}$ 168.4(3)°. Typical distances [Fe–$C_{average}$ 2.029 Å] and angles are observed for the ferrocenyl unit.[30]

$[Cu(L^3)Cl_2]$. This complex, Fig. 3, displays a slightly distorted square pyramidal geometry [τ 0.24, α 175.2(1)°, β 160.8(1)°]. The base of the square pyramid is formed by the two chloride ions [Cu–Cl 2.286(1) and 2.278(1) Å] and two of the nitrogen atoms in the tacn ring [Cu–N3 2.099(3)Å, Cu–N2 2.125(3) Å]. The other nitrogen atom (N1) forms the

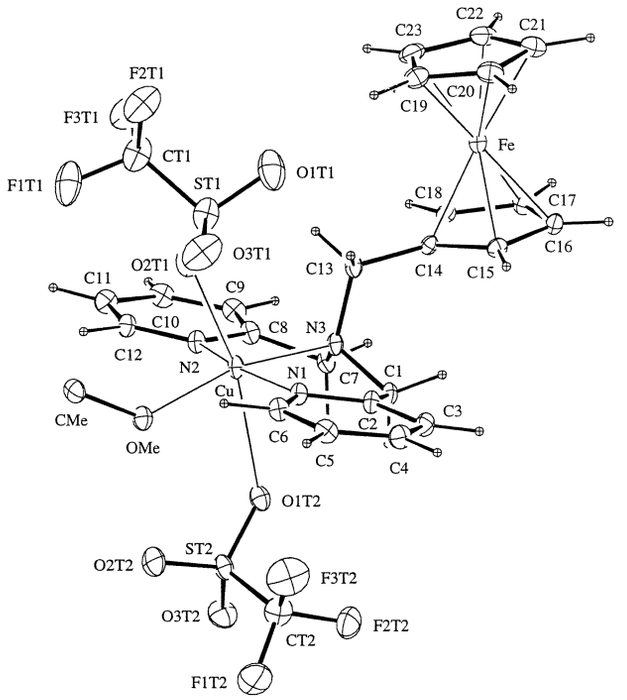

Fig. 2 View of $[Cu(L^2)(OTf)_2(CH_3OH)]$ (10% thermal ellipsoids at 294 K).

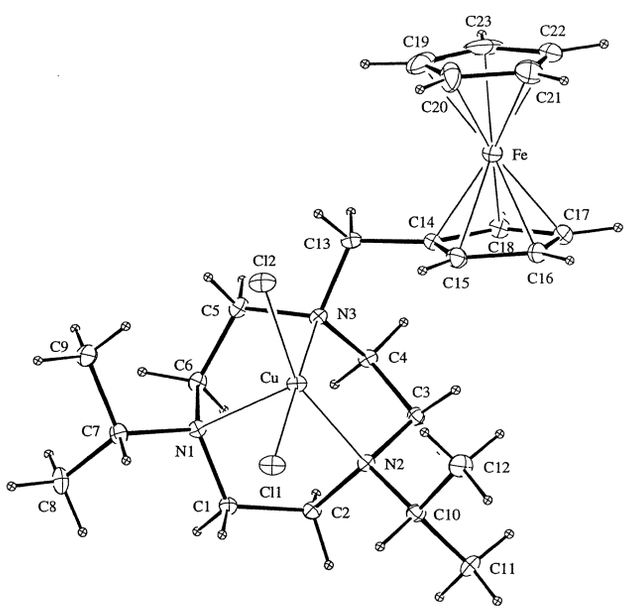

Fig. 3 View of $[Cu(L^3)Cl_2]$ (10% thermal ellipsoids at 294 K).

apex [Cu–N1 2.272(3) Å]. The metrical parameters for the copper[12–17,27–29] and ferrocenyl[30] moieties (Fe–$C_{average}$ 2.025 Å) are unexceptional.

$[\{(L^3)Cu\}_2(\mu\text{-}OH)_2](OTf)_2\cdot 0.5Et_2O$. Bright green crystals of this complex crystallised directly from a methanol solution of L^3 and copper(II) trifluoromethanesulfonate placed under a diethyl ether atmosphere. Fig. 4 gives a view of the centrosymmetric, hydroxy-bridged, dimeric cation $[\{(L^3)Cu\}_2(\mu\text{-}OH)_2]^{2+}$. Each ferrocene centre shows normal bond distances [Fe–$C_{average}$ 2.014 Å] and angles[30] and each copper exhibits a distorted square pyramidal geometry [τ 0.22; α 174.4(4)°, β 161.4(3)°]. The base of the square pyramid is formed by the two bridging oxygen atoms [Cu–O 1.960(7) and 1.946(7) Å] and two of the nitrogen atoms in the tacn ring [Cu–N3 2.086(9) Å, Cu–N2 2.065(9) Å]. The other nitrogen atom is further away and forms the apex of the square pyramid [Cu–N1 2.274(9) Å]. The two copper ions are separated by 3.017(3) Å, and the Cu–O–Cu angle is 101.1(3)°. The structure of the $(N_3)_2Cu_2(\mu\text{-}OH)_2$ core is very similar to that in $[(BzPr^i_2tacn)_2Cu_2(\mu\text{-}OH)_2]^{2+}$ ($BzPr^i_2tacn$ = 1-benzyl-4,7-diisopropyl-1,4,7-triazacyclononane) recently reported by Tolman and co-workers.[17b]

At the level of precision attained in the refinement of the crystal structure an alternative model for the dimeric cation needs to be considered, namely the dimer $[\{(L^3)Cu\}_2(\mu\text{-}O)_2]^{2+}$, with ligand L^3 in its oxidised, ferrocenium (Fe^{III}) state and two oxo ligands bridging the two copper(II) ions. We discount this alternative for three reasons. Firstly, the magnetic susceptibility of the dimer (μ_{eff}/Cu = 1.1 μ_B) is inconsistent with Cu^{II} and Fe^{III} centres. Secondly, the Vis-NIR spectrum of the complex, Fig. 5(*c*), shows a broad peak at 638 nm (ε = 130 M^{-1} cm^{-1}), very similar to that of $[(BzPr^i_2tacn)_2Cu_2(\mu\text{-}OH)_2]^{2+}$ which exhibits a peak at 640 nm (ε = 150 M^{-1} cm^{-1}).[17b] Thirdly, whilst hydroxy-bridged copper(II) dimers are relatively common,[17b,31] we are not aware of any oxo-bridged copper(II) dimers with a $[Cu_2(\mu\text{-}O)_2]$ core and it is hard to suggest why one should form here.

Physicochemical properties

Acetonitrile solutions of the ferrocenyl-copper complexes were characterised by molar conductivity measurements, by electronic absorption (Vis-NIR) and EPR spectroscopies, and by cyclic voltammetry experiments; data appear in Tables 2 and 4.

Conductivity. The molar conductivities of acetonitrile solutions of the complexes (1.0 mM) were measured. $[Cu(L^1)Cl_2]$ exhibits a low molar conductivity (Λ_M = 18 S cm^2 mol^{-1}) compared to the 1 : 1 electrolyte tetrabutylammonium hexafluorophosphate (Λ_M = 157 S cm^2 mol^{-1}), indicating that dissociation of the chloride ions is not significant in acetonitrile solution. $[Cu(L^1)Br_2]$ exhibits a higher molar conductivity value (Λ_M = 50 S cm^2 mol^{-1}) suggestive for some dissociation of the bromide ions. Similar data are observed for the molar conductivities of the other $[Cu(L)X_2]$ (X = Cl, Br) complexes, Table 2. The molar conductivity of $[Cu(L^1)(H_2O)_2](OTf)_2$ (Λ_M = 275 S cm^2 mol^{-1}) is almost twice that of a 1 : 1 electrolyte, consistent with dissociation of the trifluoromethanesulfonate ions to afford $[Cu(L^1)(solv)_n]^{2+}$ (solv = MeCN or H_2O in acetonitrile solution). It is anticipated that this species is five- or six-coordinate, bound by two or three solvent molecules. This result clearly demonstrates the weakly-coordinating nature of the trifluoromethanesulfonate anion, compared to the chloride or bromide anions. For this reason, in the ensuing discussion the copper(II) trifluoromethanesulfonate complexes are formulated as $[Cu(L)(solv)_n]^{2+}$ in order to better represent their true nature in solution.

Vis-NIR spectroscopy. Electronic absorption spectra (300–2000 nm) of the complexes were recorded in acetonitrile solution, Table 2. The spectra of the $[Cu(L)X_2]$ (L = L^1, L^2; X = Cl, Br) complexes [Fig. 5(a) and (b)] are similar, revealing a prominent ligand-centred absorbance band at ~440 nm on a rising UV-tail and a copper(II) d–d band between 740 and 800 nm with a shoulder to lower energy at ~1000 nm, an absorption profile characteristic of square pyramidal copper(II) complexes.[12–17,27,32] The copper(II) d–d bands of $[Cu(L^3)Cl_2]$ (λ_{max} = 727 nm and 1183 nm) appear to lower energy than those of $[\{(L^3)Cu\}_2(\mu\text{-}OH)_2](OTf)_2$ (λ_{max} = 638 nm and 977 nm) [Fig. 5(c)] in accord with the relative positions of the co-ligands in the spectrochemical series; again both spectra are indicative of square pyramidal copper(II) centres. Vis-NIR spectra of the $[Cu(L)(solv)_n]^{2+}$ complexes (L = L^1, L^2) [recorded in acetonitrile or in tetrahydrofuran solution] are also consistent with square pyramidal copper centres (Fig. 6). The spectrum of $[Cu(L^1)(solv)_n]^{2+}$ in acetonitrile is anomalous, showing a sharp and relatively intense peak at 628 nm. Full discussion of this is deferred until the spectra of the ferrocenium derivatives of the complexes have been described.

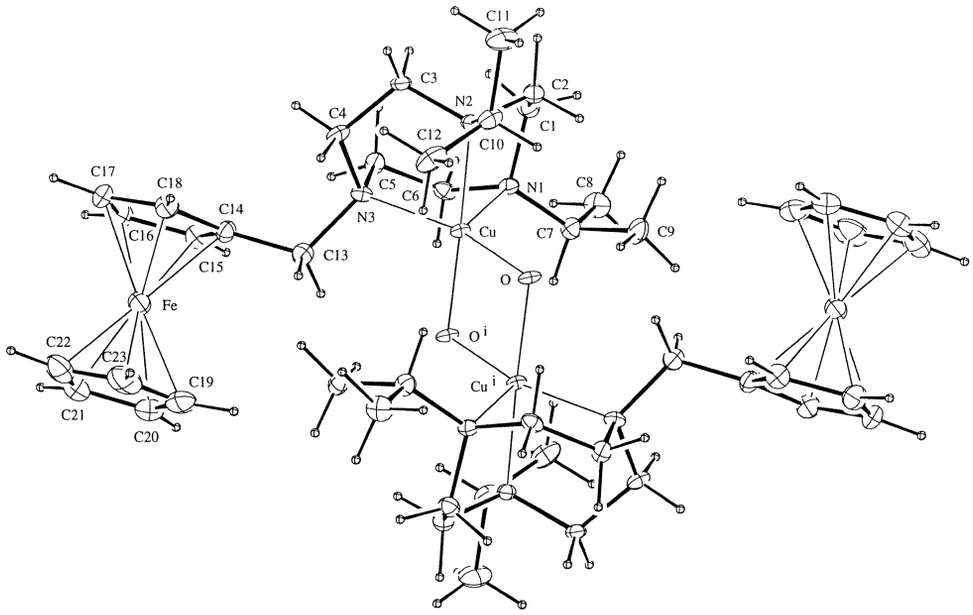

Fig. 4 View of the $[\{(L^3)Cu\}_2(\mu\text{-}OH)_2]^{2+}$ cation (10 % thermal ellipsoids at 294 K).

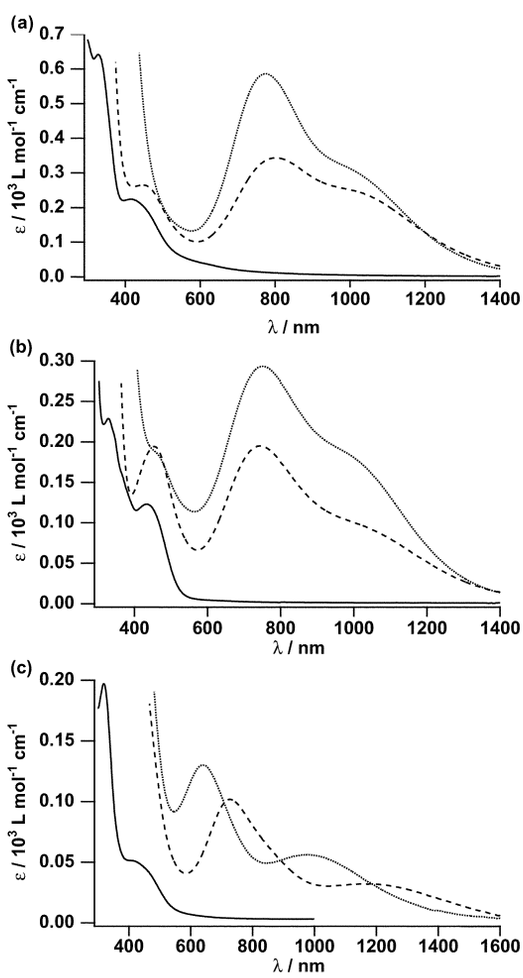

Fig. 5 Vis-NIR spectra of: (a) L^1 (—), $[Cu(L^1)Cl_2]$ (---), and $[Cu(L^1)Br_2]$ (· · ·); (b) L^2 (—), $[Cu(L^2)Cl_2]$ (---), and $[Cu(L^2)Br_2]$ (· · ·); (*c*) L^3 (—), $[Cu(L^3)Cl_2]$ (---), and $[\{(L^3)Cu\}_2(\mu\text{-}OH)_2](OTf)_2$ (· · ·). Conditions: acetonitrile, 295 K.

EPR spectroscopy. The EPR spectra of the copper(II) complexes in frozen acetonitrile solutions at 77 K are axial ($g_\parallel \sim 2.22$–$2.27 > g_\perp$ 2.05–2.12, $A_\parallel = 147$–180 G) and consistent with the above assignment of square pyramidal solution state structures;[12–17,27–29,32] representative spectra are shown in Fig. 7.

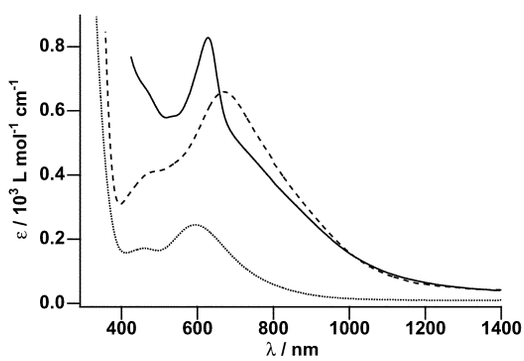

Fig. 6 Vis-NIR spectra at 295 K of $[Cu(L^1)(H_2O)_2](OTf)_2$ in dioxygen-free acetonitrile (—) and air-saturated tetrahydrofuran (---), and $[Cu(L^2)(H_2O)_2](OTf)_2$ in acetonitrile (· · ·).

For the two copper(II) bromide complexes, only broad isotropic signals were observed (at $g = 2.19$ for $[Cu(L^1)Br_2]$, and at $g = 2.11$ for $[Cu(L^2)Br_2]$). The EPR spectra of solid $[Cu(L^1)Cl_2]$ and $[Cu(L^1)Br_2]$ dispersed in KBr matrices are axial, with $g_\parallel = 2.19$ and $2.18 > g_\perp = 2.11$ and 2.12. Hyperfine coupling is not observed in these solid-state EPR spectra because the samples are not magnetically dilute. Interestingly, the EPR spectrum of microcrystalline $[Cu(L^1)(H_2O)_2](OTf)_2$ reveals an 'inverted' axial pattern ($g_\perp = 2.18 > g_\parallel = 2.08$) typical of a trigonal bipyramidal copper(II) centre, whereas the EPR spectrum of the complex in acetonitrile glass is axial, typical of an elongated octahedral or square pyramidal solution structure. No EPR signal was observed for $[\{(L^3)Cu\}_2(\mu\text{-}OH)_2](OTf)_2$ in acetonitrile glass at 77 K, suggesting that the bridging hydroxy ligands provide a pathway for antiferromagnetic coupling between the two copper centres. A magnetic moment measurement on the microcrystalline complex at 295 K gave μ_{eff}/Cu = 1.1 μ_B, also consistent with significant antiferromagnetic coupling between the two copper centres in the cation. Other $(LCu)_2(\mu\text{-}OH)_2$ complexes give similar magnetic moments and are likewise EPR silent.[17b,31]

Cyclic voltammetry. Relevant data are summarised in Table 4, and Fig. 8 displays typical CVs. The CVs of each complex exhibit a reversible ferrocene–ferrocenium (Fe^{III}–Fe^{II}) couple and, at more negative potential, a quasireversible Cu^{II}–Cu^{I} couple [$\Delta E_p(Cu^{II}$–$Cu^{I}) \approx 120$–200 mV compared to $\Delta E_p(Fe^{III}$–Fe^{II}; complex) $\approx \Delta E_p(Fc^+$–Fc; ferrocene standard) ≈ 60–70 mV].

Table 4 Potential data[a] for the ferrocenyl ligands and copper complexes, and calculated values for the relative binding constants (K_{ox}/K_{red}) and electron transfer equilibrium constants (K_{ET})

	$E_{1/2}$ (Fe^{III}–Fe^{II})/V[b]	$E_{1/2}$ (Cu^{II}–Cu^{I})/V[b]	ΔE_{Fc}/mV[c]	K_{ox}/K_{red}	$\Delta E_{Cu,Fc}$/mV[d]	K_{ET}
L^1	−0.028					
$[Cu(L^1)Cl_2]$	0.082	−0.276	110	1.4×10^{-2}	−349	1.3×10^{-6}
$[Cu(L^1)Br_2]$	0.107	−0.158	135	5.3×10^{-3}	−265	3.3×10^{-5}
$[Cu(L^1)(H_2O)_2](OTf)_2$	0.147	0.044	175	1.1×10^{-3}	−103	1.8×10^{-2}
	0.064[e]	−0.191[e]	92[e]	2.5×10^{-2}[e]	−255[e]	4.9×10^{-5}[e]
L^2	−0.008					
$[Cu(L^2)Cl_2]$	0.128	−0.580	136	5.0×10^{-3}	−708	1.1×10^{-12}
$[Cu(L^2)Br_2]$	0.138	−0.491	146	3.4×10^{-3}	−629	2.3×10^{-11}
$[Cu(L^2)(H_2O)_2](OTf)_2$	0.170	−0.231	178	1.0×10^{-3}	−401	1.7×10^{-7}
L^3	0.008					
$[Cu(L^3)Cl_2]$	0.036	−0.320	28	3.3×10^{-1}	−356	9.6×10^{-7}

[a] From cyclic voltammetry experiments; conditions: 1 mM ligand or complex in 0.1 M $NBu^n_4PF_6$–acetonitrile (except where indicated otherwise), T = 295 K, 1 mm Pt disk working electrode, scan rate = 100 mV s^{-1}. [b] Potentials are ±5 mV and are quoted relative to the ferrocenium–ferrocene couple. [c] Defined by eqn. 3 (see text). [d] Defined by eqn. 2 (see text). [e] 0.4 M $NBu^n_4PF_6$–Tetrahydrofuran.

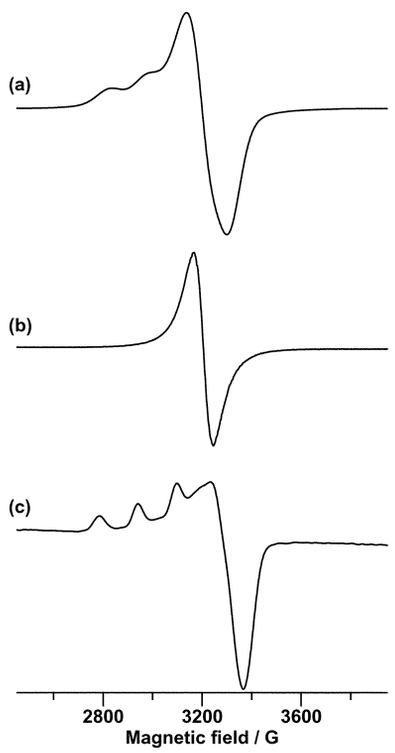

Fig. 7 EPR spectra of $[Cu(L^1)Cl_2]$ (a), $[Cu(L^1)Br_2]$ (b), and $[Cu(L^1)(H_2O)_2](OTf)_2$ (c) in frozen acetonitrile solution at 77 K.

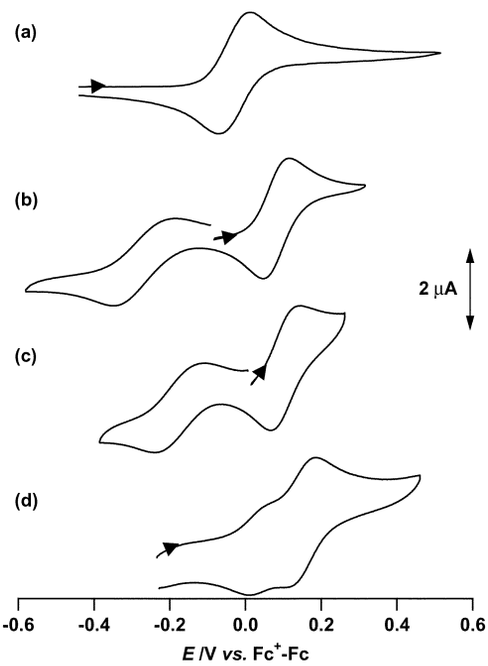

Fig. 8 Cyclic voltammograms of L^1 (a), $[Cu(L^1)Cl_2]$ (b), $[Cu(L^1)Br_2]$ (c) and $[Cu(L^1)(solv)_n]^{2+}$ (d). Conditions: 1 mM complex in 0.1 M $NBu^n_4PF_6$–acetonitrile, 295 K, 1 mm Pt disk working electrode, scan rate 100 mV s^{-1}.

Reversible ferrocene-centred couples are expected for the complexes, and Cu^{II}–Cu^{I} couples in analogous copper complexes are typically electrochemically quasireversible processes[33] because of the accompanying rate-limiting structural changes. The assignments as ferrocene- or copper-centred couples were confirmed by spectroscopic characterisation of the one-electron oxidation products (see below).[34]

Some clear trends can be discerned from the potential data in Table 4 for the two redox couples for each complex [$E_{1/2}$ (Fe^{III}–Fe^{II}) and $E_{1/2}$ (Cu^{II}–Cu^{I})] and the separation between them ($\Delta E_{Cu,Fe}$, eqn. 2).

$$\Delta E_{Cu,Fe} = E_{1/2}\,(Cu^{II}\text{–}Cu^{I}) - E_{1/2}\,(Fe^{III}\text{–}Fe^{II}) \qquad (2)$$

Consider the following series: free ligand, copper(II) chloride complex, copper(II) bromide complex, copper(II) trifluoromethanesulfonate complex. Moving along this series for a particular ligand, $E_{1/2}$ (Cu^{II}–Cu^{I}) shifts to more positive values, indicating that the copper(II) centre becomes more easily reduced. Also, along the series $E_{1/2}$ (Fe^{III}–Fe^{II}) moves to more positive values, indicating that the ferrocene centres become more difficult to oxidise. The shift in $E_{1/2}$ (Cu^{II}–Cu^{I}) is greater than that in $E_{1/2}$ (Fe^{III}–Fe^{II}), and consequently the magnitude of $\Delta E_{Cu,Fe}$ decreases along the series. The large positive shift in the Fe^{III}–Fe^{II} couple upon coordination of a copper(II) ion to each ligand makes good sense—simple electrostatics indicates that it should be easier to oxidise the ferrocene centre in the free ligand, rather than once it is complexed to the positively charged copper(II) ion. The small positive shifts of the Fe^{III}–Fe^{II} couple and the large positive shifts of the Cu^{II}–Cu^{I} couple on going from chloro co-ligands to bromo co-ligands to trifluoromethanesulfonate counter ions are consistent with the copper centre becoming increasingly positively charged. This concurs with the conductivity data (Table 2), which indicate that the degree of co-ligand dissociation in the complexes (and thus the overall charge of the copper centre) increases along the series: copper(II) chloride complex < copper(II) bromide complex < copper(II) trifluoromethanesulfonate complex.

$[\{(L^3)Cu\}_2(\mu\text{-}OH)_2](OTf)_2$ has a different CV to those of the other (monomeric) complexes, but one consistent with its dimeric structure, Fig. 9. The two ferrocene centres in

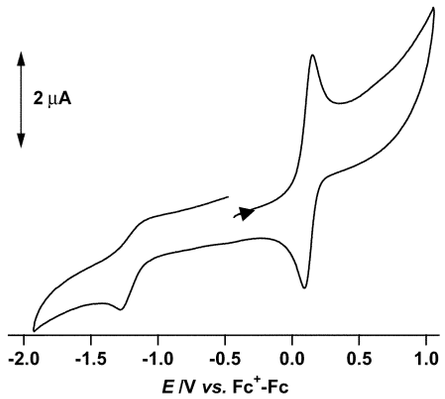

Fig. 9 Cyclic voltammogram of $[\{(L^3)Cu\}_2(\mu\text{-}OH)_2](OTf)_2$. Conditions as for Fig. 8.

$[\{(L^3)Cu\}_2(\mu\text{-}OH)_2](OTf)_2$ are separated by about 13.6 Å and cannot communicate with each other (in an electrochemical sense), leading to only one Fe^{III}–Fe^{II} couple being observed; that is, the Fe^{III}–Fe^{II} couples for each centre are coincident (at +0.12 V). The two copper centres, however, are much closer together (about 3.0 Å apart) and directly linked by bridging hydroxy ligands, and thus redox change at one copper centre will influence the other. Therefore, the single poorly-reversible, one-electron reduction process observed at −1.17 V is attributed to the irreversible reduction of the $Cu^{II}_2(\mu\text{-}OH)_2$ core.

Ferrocenium–copper (Fe^{III} ~ Cu^{II}) complexes

Oxidation of the ferrocenyl–copper(II) (Fe^{II} ~ Cu^{II}) complexes with one equivalent of ceric ammonium nitrate in acetonitrile solution gave the ferrocenium–copper(II) (Fe^{III} ~ Cu^{II}) complexes. In each of these reactions, a characteristic colour change was observed within a few seconds, typically from a pale green to an intense dark blue/green. Several of the oxidised (Fe^{III} ~ Cu^{II}) complexes displayed lifetimes of less than twelve hours; consequently, the characterisation of all oxidised complexes by Vis-NIR and EPR spectroscopies was conducted immediately.[35] Ferrocenium ion, formed by oxidation of ferrocene under the same conditions, is indefinitely stable. The free ligands L^1–L^3 were also treated with one equivalent of ceric ammonium nitrate. Intense dark blue solutions formed, characteristic of ferrocenium cations, but these decomposed within a few seconds to unknown brown mixtures thus preventing their characterisation. The decomposition of the oxidised free ligands is attributed to nucleophilic attack on the ferrocenium centre by the nitrogen-donor ligand domain. It has been long known that ferrocenium ion is decomposed by nucleophilic reagents including chloride and bromide ions and (chelating) pyridine ligands.[36]

Vis-NIR spectra of the ferrocenium–copper(II) (Fe^{III} ~ Cu^{II}) complexes all show a characteristic sharp and intense peak [compared to the broad copper(II) d–d band] between 630 and 640 nm. This peak is diagnostic for ferrocenium (Fe^{III}) ion and is ascribed to the symmetry-allowed e_{1u} (Cp) ⟶ e_{2g} (Fe) charge transfer transition.[25] The broad copper(II) d–d bands in the Fe^{III} ~ Cu^{II} species are slightly shifted to higher energy (by ~ 20–25 nm) compared to those of the parent Fe^{II} ~ Cu^{II} complexes. For example, Fig. 10 shows the electronic spectra of an acetonitrile solution of $[Cu(L^1)Cl_2]$, before (the Fe^{II} ~ Cu^{II} complex) and after (the Fe^{III} ~ Cu^{II} complex) oxidation with one equivalent of ceric ion. Adding extra ceric ion had no effect on the absorbance of the ferrocenium band but did cause some broadening of the copper(II) d–d bands, possibly due to accelerated decomposition of the Fe^{III} ~ Cu^{II} complex. The EPR spectra of acetonitrile glasses (77 K) of the oxidised (Fe^{III} ~ Cu^{II}) complexes show weak signals from residual Fe^{II} ~ Cu^{II} complex that are 10^2 to 10^3 times less intense than the signal

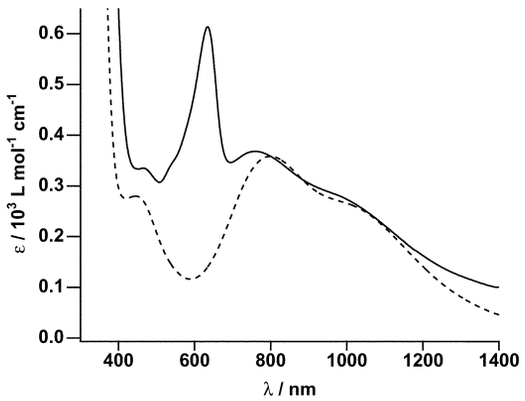

Fig. 10 Vis-NIR spectra of $[Cu(L^1)Cl_2]$ in acetonitrile at 295 K before (Fe^{II} ~ Cu^{II} state: ---) and after (Fe^{III} ~ Cu^{II} state: —) addition of one equivalent of ceric ion.

prior to addition of the ceric ion. The EPR silence of the Fe^{III} ~ Cu^{II} species is attributed to the close proximity of the ferrocenium and copper(II) centres, and perhaps results from fast dipolar relaxation as is commonly found for many bis(transition metal) diradicals.[37] It is clear from these spectroscopic results—the similarity of the copper d–d bands before and after oxidation, and the EPR silence of the oxidised material—that the copper(II) centre remains bound to the ligand after oxidation (that is, replacement of copper by cerium does not occur).

The relatively short lifetimes of the oxidised (Fe^{III} ~ Cu^{II}) complexes are readily explained by considering the complexation equilibria for the oxidised and reduced states of ligands L^1–L^3, Scheme 1.[38] The observed shift in the potential for the

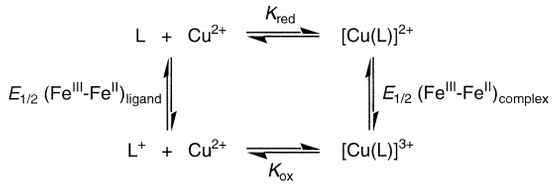

Scheme 1

ferrocenyl Fe^{III}–Fe^{II} couple (ΔE_{Fc}) upon complexation by copper(II) ion allows the relative copper(II) binding constants for the oxidised (K_{ox}) and reduced (K_{red}) states of the ligand to be calculated, according to eqns. 3 and 4.

$$\Delta E_{Fc} = E_{1/2}\,(Fe^{III}\text{–}Fe^{II})_{complex} - E_{1/2}\,(Fe^{III}\text{–}Fe^{II})_{free\ ligand} \quad (3)$$

$$\Delta E_{Fc} = -\,(RT/nF)\,\ln(K_{ox}/K_{red}) \quad (4)$$

The data (Table 4) indicate that the copper(II) ions are 10^2–10^3 times less strongly bound in the oxidised species. This behaviour is expected [38] and is due to the combined effects upon oxidation to afford the Fe^{III} ~ Cu^{II} species of the increased electrostatic repulsion between the transition metal centres, the increased inductive electron withdrawal from the copper-binding domain by the ferrocenium centre, and the increased attraction of the ferricenium centre for the ligands about the copper centre. Dissociation of the more weakly bound copper(II) ion in the Fe^{III} ~ Cu^{II} state will give free oxidised ligand, which rapidly decomposes by the aforementioned pathway.

$[Cu(L^1)(H_2O)_2](OTf)_2$: Evidence for an Fe^{II} ~ Cu^{II} ⇌ Fe^{III} ~ Cu^{I} equilibrium

The impetus for further investigation of $[Cu(L^1)(H_2O)_2](OTf)_2$ came from a simple observation. Acetonitrile solutions of the complex are air-sensitive and rapidly change colour from bright

blue to brown–green when exposed to the atmosphere, whereas the solid and solutions of the complex in other solvents (such as dichloromethane or tetrahydrofuran) are indefinitely stable in air. In order to study this behaviour, Vis-NIR spectra of $[Cu(L^1)(solv)_n]^{2+}$ were recorded at several concentrations (from 0.2–5 mM) in anhydrous acetonitrile under dinitrogen and in tetrahydrofuran in air, Fig. 6. The spectra were independent of concentration. In tetrahydrofuran, a broad copper(II) d–d band at 671 nm is observed and, noteworthily, there is no hint of a ferrocenium peak. In contrast, in acetonitrile the spectrum is dominated by a relatively sharp and intense peak at 628 nm. Comparison of this spectrum with those of the fully oxidised $Fe^{III} \sim Cu^{II}$ state (*e.g.* Fig. 10) indicates that the peak may be ascribed to the characteristic charge transfer transition in the ferrocenium (Fe^{III}) ion; the broad, lower intensity shoulder to lower energy, Fig. 6, is assigned to the copper(II) d–d band(s). The question arises, where does the ferrocenium ion come from? The magnetic moment of $[Cu(L^1)(H_2O)_2](OTf)_2$ ($\mu = 2.1$ μ_B) suggests that the presence of ferrocenium ion in the solid sample is unlikely. To confirm this we obtained the Mössbauer spectrum of the microcrystalline bulk sample, Fig. 11, which

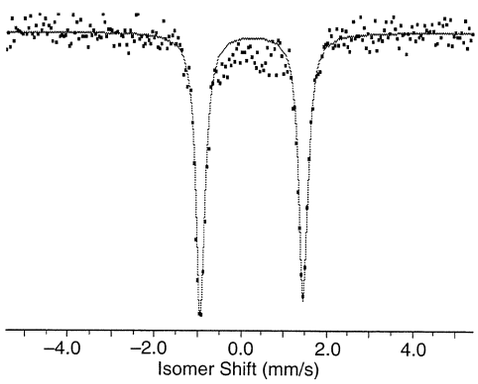

Fig. 11 ^{57}Fe Mössbauer spectrum of bulk sample of $[Cu(L^1)(H_2O)_2](OTf)_2$ at 295 K.

reveals a typical doublet with an isomer shift (0.44 mm s^{-1}) and a quadrupole splitting (2.38 mm s^{-1}) indicative for a single ferrocenyl (Fe^{II}) centre.[39] Microcrystalline $[Cu(L^1)(H_2O)_2](OTf)_2$ exists exclusively in the $Fe^{II} \sim Cu^{II}$ state, and the ferrocenium (Fe^{III}) ion, observed in the electronic spectrum of the complex in acetonitrile, must be generated in solution.

When a dark blue solution of $[Cu(L^1)(solv)_n]^{2+}$ in acetonitrile was bubbled with dry dioxygen at room temperature, the colour immediately changed to a deep green. The Vis-NIR spectrum immediately after bubbling with dioxygen showed a 2.4-fold increase in the absorbance of the sharp 628 nm ferrocenium band. The lower energy shoulder corresponding to the copper d–d band(s) was little changed. The ferrocenium species is not stable—over several hours the ferrocenium band weakened and then disappeared and, at the same time, brown insoluble material precipitated. These results reveal $[Cu(L^1)(solv)_n]^{2+}$, which is entirely copper(II) in the solid sample and stable in tetrahydrofuran solution, to react with dioxygen in acetonitrile solution.

There are two possibilities for the production of the ferrocenium ion by dioxygen: (1) Dioxygen directly oxidises the ferrocenyl centre in $[Cu(L^1)(solv)_n]^{2+}$. This is discounted for the following reasons. First, the Fe^{III}–Fe^{II} couples of the complexes are all positive of that for ferrocene which is not oxidised by dioxygen, except under strongly acidic conditions.[40] Even 1,1′-dimethylferrocene [$E_{1/2}(Fe^{III}–Fe^{II}) = -0.11$ V] in acetonitrile solution, with a Fe^{III}–Fe^{II} couple 260 mV lower than that for $[Cu(L^1)(solv)_n]^{2+}$, is not directly oxidised by dioxygen.[40] Secondly, whilst solutions of $[Cu(L)(solv)_n]^{2+}$ (L = L^1, L^2; solv = solvent or H_2O) may be slightly acidic due to polarisation of water co-ligands, neither $[Cu(L^2)(solv)_n]^{2+}$ in acetonitrile solution nor $[Cu(L^1)(solv)_n]^{2+}$ itself in tetrahydrofuran or dichloromethane solutions are oxidised by dioxygen. Thirdly, direct oxidation does not account for the ferrocenium bands observed for the dioxygen-free, acetonitrile solutions of $[Cu(L^1)(solv)_n]^{2+}$ (dioxygen levels were less than 2 ppm in the glove-box employed for preparing the solutions). (2) An intramolecular electron transfer equilibrium exists in acetonitrile solution between $Fe^{II} \sim Cu^{II}$ and $Fe^{III} \sim Cu^{I}$ valence tautomers, eqn. 5: The presence

$$Fe^{II} \sim Cu^{II} \rightleftharpoons Fe^{III} \sim Cu^{I} \quad (5)$$

of the $Fe^{III} \sim Cu^{I}$ tautomer of $[Cu(L^1)(solv)_n]^{2+}$ in acetonitrile solution neatly accounts for the ferrocenium (Fe^{III}) band in the Vis-NIR spectra and the reaction with dioxygen, typical of a copper(I) species, leading to an unstable $Fe^{III} \sim Cu^{II}$ product. For $[Cu(L^1)(solv)_n]^{2+}$, the electron transfer equilibrium would be accompanied by changes to the coordination of copper—Cu^{I}(bpea) centres are consistently found to have three-coordinate copper(I) ions bound only by the two pyridyl and amine groups of the bpea ligand in a T-shaped arrangement or four-coordinate copper(I) ions bound by the bpea ligand and a weakly bound solvent or anion co-ligand.[16] It is well established that the copper(I) complexes of bpea ligands bind dioxygen at low temperatures to afford dinuclear Cu_2O_2 adducts which cleanly decompose to copper(II)–hydroxo species upon warming, whereas the copper(II) complexes are inert towards dioxygen.[15,16,41] Hence, $Fe^{III} \sim Cu^{II}$ products with hydroxo co-ligands are expected from the reaction of the $Fe^{III} \sim Cu^{I}$ tautomer with dioxygen at ambient temperature. Such $Fe^{III} \sim Cu^{II}$ species should be unstable, due to weaker binding and dissociation of copper (see above) and also because the hydroxide co-ligand(s) may attack the ferrocenium centre causing its decomposition.[36]

Consideration of the redox potentials for the ferrocenyl–copper complexes (Table 4) indicates why an intramolecular electron transfer equilibrium should be observed for $[Cu(L^1)(solv)_n]^{2+}$ in acetonitrile, and not for the other complexes. As the potential of the Cu^{II}–Cu^{I} couple approaches that of the Fe^{III}–Fe^{II} couple (*i.e.*, as the magnitude of $\Delta E_{Cu,Fe}$ declines), the likelihood of electron transfer between the copper and ferrocene centres increases. The smallest $\Delta E_{Cu,Fe}$ value is observed for $[Cu(L^1)(solv)_n]^{2+}$ in acetonitrile solution (−103 mV) and intramolecular electron transfer is most likely for this complex. The other complexes have $\Delta E_{Cu,Fe}$ values with magnitudes > 250 mV. Intramolecular electron transfer is too endoergic to be observed and consequently the other complexes show no ferrocenium peak in their electronic spectra and do not react with dioxygen.

An intramolecular electron transfer leading to the $Fe^{II} \sim Cu^{II}$ and $Fe^{III} \sim Cu^{I}$ valence tautomers [equilibrium constant (K_{ET})] can be written as the sum of the two one-electron steps in Scheme 2. The relationships between the redox potentials and K_{ET} are given by eqns. 6–9.

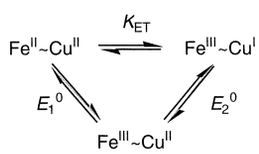

Scheme 2

$$\Delta G^\circ = -RT \ln K_{ET} = -nF\Delta E^\circ \quad (6)$$

$$K_{ET} = [Fe^{III} \sim Cu^{I}]/[Fe^{II} \sim Cu^{II}] \quad (7)$$

$$\Delta E^\circ = E_2^\circ - E_1^\circ \quad (8)$$

$$\Delta E^\circ = (RT/nF) \ln K_{ET} \quad (9)$$

$E_1°$ is the potential of the Fe^{III}–Fe^{II} couple for the complex [*i.e.*, $E_{1/2}$ (Fe^{III}–Fe^{II})], and for $[Cu(L^1)(solv)_n]^{2+}$ is +147 mV. $E_2°$ is the potential of the Cu^{II}–Cu^{I} couple with the ligand in its oxidised (Fe^{III}) state and cannot be measured, because the Cu^{II}–Cu^{I} couple occurs to a more negative potential than the Fe^{III}–Fe^{II} couple in the complexes. However, a conservative estimate of $E_2°$ may be obtained from the potential of the Cu^{II}–Cu^{I} couple with the ligand in its reduced (Fe^{II}) state, which can be measured—$E_2°_{est}$ is $E_{1/2}$ (Cu^{II}–Cu^{I}) and is +44 mV for $[Cu(L^1)(solv)_n]^{2+}$. Thus $\Delta E_{Cu,Fe}$ for $[Cu(L^1)(solv)_n]^{2+}$ at −103 mV is used as an estimate for $\Delta E°$, leading to a value for K_{ET} of 1.8×10^{-2}; that is, the 103 mV separation between the Cu^{II}–Cu^{I} and Fe^{III}–Fe^{II} couples corresponds to *at least* 2 % Fe^{III} ~ Cu^{I} tautomer of $[Cu(L^1)(solv)_n]^{2+}$ in acetonitrile solution. It is important to realise that $E_2°_{est}$ is lower than $E_2°$ because the reduction of the copper(II) centre will always be easier with a ferrocenium substituent (by both inductive and electrostatic arguments[38]). Therefore, the above calculation will considerably underestimate the concentration of the Fe^{III} ~ Cu^{I} tautomer.

Cyclic voltammograms of $[Cu(L^1)(solv)_n]^{2+}$ reveal $E_{1/2}$(Cu^{II}–Cu^{I}) shifts negative in tetrahydrofuran compared to in acetonitrile. Tetrahydrofuran, unlike acetonitrile, does not solvate copper(I) species particularly strongly,[42] leading to the increased relative stability for the copper(II) state. As a result $\Delta E_{Cu,Fe}$ is more uphill (−255 mV) in tetrahydrofuran solution and the equilibrium between the valence tautomers (eqn. 5) lies far to the left ($K_{ET} = 4.9 \times 10^{-5}$). Consequently, the electronic spectrum of $[Cu(L^1)(solv)_n]^{2+}$ in tetrahydrofuran shows no ferrocenium peak, Fig. 6, and the complex does not react with dioxygen. The result corroborates the conclusion that the reactivity of the complex towards dioxygen in acetonitrile solution arises from the intramolecular electron transfer equilibrium, eqn. 5.

Possible biological relevance

First and foremost, the present study demonstrates that an electron transfer equilibrium between adjacent copper and auxiliary electron donor centres, akin to that found in CAOs, can lead to the copper centre (as the Cu^{I} tautomer) reacting with dioxygen.

Secondly, the logarithmic relationship for K_{ET}, eqn. 9, ensures that an equilibrium between valence tautomers will only be observable when the Cu^{I}–Cu^{II} couple and that of the auxiliary electron donor are closely matched (to within ≈ ±150 mV of each other). Therefore the Cu^{II}–Cu^{I} and the cofactor aminosemiquinone–aminohydroquinone couples in the substrate-reduced state of CAOs must be closely matched, *with the Cu^{II}–Cu^{I} couple being the lower* in substrate-reduced BSAO since the Cu^{II} ~ aminohydroquinone state predominates in the electron-transfer equilibrium.[9] If the aminohydroquinone is capable of transferring one electron directly to dioxygen in the first step of the oxidative phase of the BSAO enzyme cycle as recently proposed,[9] then so is the copper(I) centre and with greater thermodynamic driving force. The kinetics of the respective electron transfers to dioxygen from aminohydroquinone or copper(I) will determine the actual electron donor.

Thirdly, the results highlight the crucial effect of the environment on redox behaviour and, consequently, on an electron-transfer equilibrium between adjacent copper and auxiliary electron donor centres. For example, addition of chloride ion to $[Cu(L^1)(solv)_n]^{2+}$ [$E_{1/2}$(Cu^{II}–Cu^{I}) = 0.04 V] in acetonitrile gives $[Cu(L^1)Cl_2]$ [$E_{1/2}$(Cu^{II}–Cu^{I}) = −0.28 V] and kills the reactivity with dioxygen; likewise $[Cu(L^1)(solv)_n]^{2+}$ is stable to dioxygen in tetrahydrofuran solution. Unfortunately in CAOs direct electrochemical measurements of the reduction potentials of the copper and the TOPA-quinone centres are not possible, because redox mediators cannot negotiate the narrow channel for the substrate to enter and the product to leave the buried active site.[1] Consequently the effect of the local environment of the cofactor, which varies at each step of the enzyme cycle, on its redox chemistry is unknown and therefore estimates for the aminosemiquinone–aminohydroquinone couple in substrate-reduced CAOs evaluated from models, such as those recently used to support argument for a mechanism involving direct transfer of one electron from the aminohydroquinone to dioxygen in BSAO,[9] are of questionable worth.

Conclusion

Copper(II) complexes of L^1–L^3 in their oxidised (Fe^{III}) and reduced (Fe^{II}) states have been characterised. Evidence for an electron transfer equilibrium between the Fe^{III} ~ Cu^{I} and Fe^{II} ~ Cu^{II} tautomers of one complex is presented and the factors leading to this are delineated. The Fe^{III} ~ Cu^{I} tautomer reacts with dioxygen.† Some possible implications for CAOs are mentioned. A final comment on CAOs: Given this demonstration of a copper complex that is oxidised by dioxygen as the result of an equilibrium between valence tautomers, it seems surprising that CAOs should evolve exhibiting similar electron transfer equilibria at catalytically competent rates if the copper centres in these proteins are not involved in the binding and reduction of dioxygen.

Acknowledgements

We thank Professor H. A. Goodwin for the Mössbauer spectrum and Dr. X.-H. Yang for some starting materials. This research was funded by the Australian Research Council.

† *Note added at proof*: A recent report describes copper complexes from 9,10-phenanthrenequinone that show valence tautomerism and react with dioxygen: G. Speier, Z. Tyeklár, P. Tóth, E. Speir, S. Tisza, A. Rockenbauer, A. M. Whalen, N. Alkire and C. G. Pierpont, *Inorg. Chem.*, 2001, **40**, 5653–5659.

References

1 J. P. Klinman, *Chem. Rev.*, 1996, **96**, 2541–2561.
2 S. M. Janes, D. Mu, D. Wemmer, A. J. Smith, S. Kaur, D. Maltby, A. L. Burlingame and J. P. Klinman, *Science*, 1990, **248**, 981–987.
3 B. Schwartz, A. K. Olgin and J. P. Klinman, *Biochemistry*, 2001, **40**, 2954–2963.
4 (*a*) M. R. Parsons, M. A. Convery, C. M. Wilmot, K. D. S. Yadav, V. Blakely, A. S. Corner, S. E. V. Phillips, M. J. McPherson and P. F. Knowles, *Structure*, 1995, **3**, 1171–1184; (*b*) V. Kumar, D. M. Dooley, H. C. Freeman, J. M. Guss, I. Harvey, M. A. McGuirl, M. C. J. Wilce and V. M. Zubak, *Structure*, 1996, **4**, 943–955; (*c*) M. C. J. Wilce, D. M. Dooley, H. C. Freeman, J. M. Guss, H. Matsunami, W. S. McIntire, C. J. E. Ruggiero, K. Tanizawa and H. Yamaguchi, *Biochemistry*, 1997, **36**, 16116–16133; (*d*) R. Li, J. P. Klinman and F. S. Mathews, *Structure*, 1998, **6**, 293–307.
5 C. M. Wilmot, J. Hajdu, M. J. McPherson, P. F. Knowles and S. E. V. Phillips, *Science*, 1999, **286**, 1724–1728.
6 (*a*) M. Mure and J. P. Klinman, *J. Am. Chem. Soc.*, 1993, **115**, 7117–7127; (*b*) F. Wang, J.-Y. Bae, A. R. Jacobson, Y. Lee and L. M. Sayre, *J. Org. Chem.*, 1994, **59**, 2409–2417; (*c*) M. Mure and J. P. Klinman, *J. Am. Chem. Soc.*, 1995, **117**, 8698–8706; (*d*) M. Mure and J. P. Klinman, *J. Am. Chem. Soc.*, 1995, **117**, 8707–8718; (*e*) S. Mandal, Y. Lee, M. M. Purdy and L. M. Sayre, *J. Am. Chem. Soc.*, 2000, **122**, 3574–3584.
7 (*a*) D. M. Dooley, M. A. McGuirl, D. E. Brown, P. N. Turowski, W. S. McIntire and P. F. Knowles, *Nature (London)*, 1991, **349**, 262–264; (*b*) P. N. Turowski, M. A. McGuirl and D. M. Dooley, *J. Biol. Chem.*, 1993, **268**, 17680–17682; (*c*) D. M. Dooley and D. E. Brown, *J. Biol. Inorg. Chem.*, 1996, **1**, 205–209; (*d*) M. A. McGuirl, D. E. Brown and D. M. Dooley, *J. Biol. Inorg. Chem.*, 1997, **2**, 336–342.
8 D. M. Dooley, R. A. Scott, P. F. Knowles, C. M. Colangelo, M. A. McGuirl and D. E. Brown, *J. Am. Chem. Soc.*, 1998, **120**, 2599–2605.
9 Q. Su and J. P. Klinman, *Biochemistry*, 1998, **37**, 12513–12525.
10 S. A. Mills and J. P. Klinman, *J. Am. Chem. Soc.*, 2000, **122**, 9897–9904.
11 J. Rall, M. A. Wanner, F. M. Hornung and W. Kaim, *Chem. Eur. J.*, 1999, **5**, 2802–2809.

12 P. Y. Li, N. K. I. Solanki, H. Ehrenberg, N. Feeder, J. E. Davies, J. M. Rawson and M. A. Halcrow, *J. Chem. Soc. Dalton Trans.*, 2000, 1559–1565.
13 C. L. Foster, X. M. Liu, C. A. Kilner, M. Thornton-Pett and M. A. Halcrow, *J. Chem. Soc. Dalton Trans.*, 2000, 4563–4568.
14 (*a*) N. Nakamura, T. Kohzuma, H. Kuma and S. Suzuki, *J. Am. Chem Soc.*, 1992, **114**, 6550–6552; (*b*) S. Suzuki, K. Yamaguchi, N. Nakamura, Y. Tagawa, H. Kuma and T. Kawamoto, *Inorg. Chim. Acta*, 1998, **283**, 260; (*c*) T. Sixt and W. Kaim, *Inorg. Chim. Acta*, 2000, **300–302**, 762–768.
15 N. Kitajima and Y. Moro-oko, *Chem. Rev.*, 1994, **94**, 737–757.
16 (*a*) K. D. Karlin, S. Kaderli and A. D. Zuberbühler, *Acc. Chem. Res.*, 1997, **30**, 139–147; (*b*) H. V. Obias, Y. Lin, N. N. Murthy, E. Pidcock, E. I. Solomon, M. Ralle, N. J. Blackburn, Y.-M. Neuhold, A. D. Zuberbühler and K. D. Karlin, *J. Am. Chem. Soc.*, 1998, **120**, 12960–12961; (*c*) E. Pidcock, H. V. Obias, M. Abe, H.-C. Liang, K. D. Karlin and E. I. Solomon, *J. Am. Chem. Soc.*, 1999, **121**, 1299–1308; (*d*) E. Pidcock, S. DeBeer, H. V. Obias, B. Hedman, K. O. Hodgson, K. D. Karlin and E. I. Solomon, *J. Am. Chem. Soc.*, 1999, **121**, 1870–1878.
17 (*a*) J. A. Halfen, S. Mahapatra, E. C. Wilkinson, S. Kaderli, V. G. Young Jr., L. Que Jr., A. D. Zuberbühler and W. B. Tolman, *Science*, 1996, **271**, 1397–1400; (*b*) S. Mahapatra, J. A. Halfen and W. B. Tolman, *J. Am. Chem. Soc.*, 1996, **118**, 11575–11586; (*c*) W. B. Tolman, *Acc. Chem. Res.*, 1997, **30**, 227–237; (*d*) P. L. Holland and W. B. Tolman, *Coord. Chem. Rev.*, 1999, **190–192**, 855–869.
18 S. B. Sembiring, S. B. Colbran and D. C. Craig, *J. Chem. Soc., Dalton Trans.*, 1999, 1543–1554.
19 V. V. Pavlishchuk and A. A. Addison, *Inorg. Chim. Acta*, 2000, **298**, 97–102.
20 D. Lednicer and C. R. Hauser, *Org. Synth.*, 1960, **40**, 31–33.
21 L. E. Brady, M. Freifelder and G. R. Stone, *J. Org. Chem.*, 1961, **26**, 4757–4760.
22 J. K. Romary, R. D. Zachariasen, J. D. Berger and H. Schiesser, *J. Chem. Soc. (C)*, 1968, 2884–2887.
23 J. A. Halfen, W. B. Tolman and K. Wieghardt, *Inorg. Synth.*, 1998, **32**, 75–81.
24 For the closely related ligand, 1-ferrocenylmethyl-1,4,7-triazacyclononane, and a nickel(II) complex of this, see G. De Santis, L. Fabbrizzi, M. Licchelli, C. Mangano, P. Pallavicini and A. Poggi, *Inorg. Chem.*, 1993, **32**, 854–860.
25 (*a*) J. E. Frey, L. E. Du Pont and J. J. Puckett, *J. Org. Chem.*, 1994, **59**, 5386–5392; (*b*) E. Rühl and A. P. Hitchcock, *J. Am. Chem. Soc.*, 1989, **111**, 5069–5075.
26 S. B. Colbran, A. J. Evans, S. E. Watkins and D. C. Craig, unpublished work.
27 A. W. Addison, T. N. Rao, J. Reedijk, J. van Rijn and G. C. Verschoor, *J. Chem. Soc. Dalton Trans.*, 1984, 1349–1356.
28 (*a*) K. D. Karlin, J. W. McKown, J. C. Hayes, J. P. Hutchinson and J. Zubieta, *Transition Met. Chem.*, 1984, **9**, 405–406; (*b*) C. Cox, D. Ferraris, N. N. Murthy and T. Lectka, *J. Am. Chem. Soc.*, 1996, **118**, 5332–5333.
29 (*a*) S. S. Tandon, L. Chen, L. K. Thompson, S. P. Connors and J. N. Bridson, *Inorg. Chim. Acta*, 1993, **213**, 289–300; (*b*) F. M. Menger, J.-J. Lee and K. S. Hagen, *J. Am. Chem. Soc.*, 1991, **113**, 4017–4019.
30 R. J. Webb, S. J. Geib, D. L. Staley, A. L. Rheingold and D. N. Hendickson, *J. Am. Chem. Soc.*, 1990, **112**, 5031–5042.
31 (*a*) D. J. Hodgson, *Prog. Inorg. Chem.*, 1975, **19**, 173–242; (*b*) N. Kitajima, S. Hikichi, M. Tanaka and Y. Moro-oka, *J. Am. Chem. Soc.*, 1993, **115**, 5496–5508.
32 B. J. Hathaway, in *Comprehensive Coordination Chemistry*, ed. G. Wilkinson, Pergamon Press, Oxford, vol. 5, 1987, ch. 53, p. 533.
33 S. J. Brudenell, L. Spiccia, A. M. Bond, P. Comba and D. C. Hockless, *Inorg. Chem.*, 1998, **37**, 3705–3713.
34 The one-electron reduction products have also been isolated and are $Fe^{II} \sim Cu^{I}$ species A. J. Evans and S. B. Colbran, unpublished work.
35 Vis-NIR (350–2000 nm) and EPR (77 K) spectra of acetonitrile solutions of ceric and cerous ions at the same concentration as used in the oxidation experiments were also recorded and show no peaks/signals.
36 (*a*) R. Prins, A. R. Korswagen and A. G. T. G. Kortbeek, *J. Organomet. Chem.*, 1972, **39**, 335–344; (*b*) J. K. Baskin and P. J. Kinlen, *Inorg. Chem.*, 1990, **29**, 4507–4509.
37 J. R. Pilbrow, *Transition Metal Electron Paramagnetic Resonance*, Oxford University Press, Oxford, 1990.
38 P. D. Beer, P. A. Gale and G. Z. Chen, *J. Chem. Soc. Dalton Trans.*, 1999, 1897–1909.
39 J. Kreisz, R. U. Kirss and W. M. Reiff, *Inorg. Chem.*, 1994, **33**, 1562–1565.
40 (*a*) S. Fukuzumi, S. Mochizuki and T. Tanaka, *Inorg. Chem.*, 1989, **28**, 2459–2465; (*b*) S. Fukuzumi, K. Ishikawa and T. Tanaka, *Chem. Lett.*, 1986, 1–4.
41 It is noteworthy that a Cu_2O_2 adduct does not oxidise ferrocene: see ref. 17(*b*).
42 (*a*) A. Lewandowski and J. Malinska, *New. J. Chem.*, 1996, **20**, 653–657; (*b*) L. Aronne, B. C. Dunn, J. R. Vyvyan, C. W. Souvignier, M. J. Mayer, T. A. Howard, C. A. Salhi, S. N. Goldie, L. A. Ochrymowycz and D. B. Rorabacher, *Inorg. Chem.*, 1995, **34**, 357–369.